Plasmon Coupling in Two-Dimensional Arrays of Silver Nanoparticles: I. Effect of the Dielectric Medium

Mark K. Kinnan,[†] Svetlana Kachan,[‡] Courtenay K. Simmons,[†] and George Chumanov*,[†]

235 Hunter Laboratories, Clemson University, Clemson, South Carolina 29634 and B. I. Stepanov Institute of Physics, 68 Nezavisimosti Avenue, 220072 Mink, Belarus

Received: January 5, 2009; Revised Manuscript Received: January 28, 2009

The effect of the dielectric medium between the particles on plasmon coupling was studied experimentally and theoretically. Two-dimensional arrays of silver nanoparticles adsorbed on glass slides were immobilized using poly(methylmethacrylate). The method provides an efficient way for stabilization of particles on surfaces. It was concluded that increasing the dielectric function of the surrounding medium promotes plasmon coupling between silver nanoparticles. On the basis of the quasi-crystalline approximation, the optimum refractive index was calculated that yielded the strongest and highest Q extinction band due to coherent plasmon coupling.

Introduction

Optical properties of silver nanoparticles (SNPs) are determined by excitation of the plasmon resonances that are the collective oscillations of the free electron density.[1] The optical excitation of plasmon resonances in SNPs represents the most efficient mechanism by which light interacts with matter. By varying the particle size, shape, and surrounding dielectric medium the plasmon resonance can be tuned across the near-UV, visible, and near-infrared spectral range. The high efficiency for interaction with light, tunability of the optical resonance, as well as photochemical robustness makes SNPs attractive for applications in optical filters,[2] plasmonic waveguides,[3] substrates for surface-enhanced spectroscopies,[4−6] and biosensors.[7,8]

Excitation of plasmon resonances produces an electromagnetic field localized around SNPs that is enhanced as compared to the incident field. Evanoff et al. reported that the local electromagnetic field extends approximately 40 nm from the surface of 84 nm diameter particles.[9] When several particles are put into close proximity so that the local fields associated with electron oscillations in individual particles overlap, the system undergoes plasmon coupling and new plasmon modes result. The plasmon coupling was observed in 2D arrays of SNPs as a sharp band in the blue spectral range of the extinction spectra representing a coherent plasmon mode.[10] Drying of these arrays changed the refractive index of the medium between the particles from that of water (1.33) to that of air (1) and resulted in a loss of the sharp band. Additionally, the drying lead to the aggregation of the SNPs due to the forces associated with the surface tension of water as it dries.[11] Malynych et al. reported that the sharp band was preserved when the arrays were embedded into the poly(dimethylsiloxane) polymer matrix.[11] Even though embedding the SNPs into polymer matrixes proved to stabilize SNPs from aggregation, the particles are covered with a polymer and their surface is not accessible to the environment—a feature desired for sensing applications of these arrays. It was previously shown that the coupled SNP arrays that are not embedded into polymers can be used for sensing of the refractive index when immersed into different solvents.[12] However, the coherent plasmon mode of the embedded arrays was insensitive to changes of the dielectric medium.

A new approach for stabilizing SNP arrays based on immobilizing the particles with a thin layer of poly(methylmethacrylate) (PMMA) was developed in this work. The key advantage of this approach relates to the ability of casting thin PMMA layers in the space between SNPs and not on their surface. This is achievable because PMMA does not wet the silver surface due to poor interaction between the two. The uncoated silver surface remained accessible to the interaction with various molecules, and this principle can be potentially utilized in sensing applications of SNP arrays. In addition, this approach allowed addressing a fundamental question about the effect of the dielectric medium on plasmon coupling.

Experimental Section

Materials. Poly(methylmethacrylate) (PMMA) [MW ≈ 996 000], anisole, 4-aminothiophenol, and poly(4-vinylpyridine) (PVP) were purchased from Sigma Aldrich. Silver(I) oxide and USP Absolute-200 Proof ethanol were acquired from Alfa Aesar and Aaper Alcohol & Chemical Co., respectively. All chemicals were used as received. Microscope glass slides were obtained from VWR. Deionized water with a nominal resistivity of 18 MΩ·cm came from a Millipore Milli-Q water purification system. Ultra-high-purity nitrogen and ultra-high-purity hydrogen were purchased from Air Gas. PMMA and PVP solutions were made by dissolving a weighed quantity of PMMA or PVP into anisole and ethanol, respectively.

Instrumentation. UV−vis absorption spectra were recorded using a Shimadzu UV-2501PC spectrophotometer. Electron microscopy images were taken with a Hitachi SEM-4800. Spin drying was performed using a spin coater WS-400B-6NPP/LITE (Laurell Technologies Corp.). Topographical images were recorded using an AutoProbe CP AFM equipped with Mikro-Masch Noncontact silicon cantilevers (NSC11/50) in noncontact mode. The AFM images were processed using MatLAB 2007b. All spectra were processed and figures prepared using SpectraSolve for Windows (LasTek Pty. Ltd.). The Feret's diameter of the particles was calculated using ImageJ for Windows (http://rsbweb.nih.gov/ij/).

Synthesis of Silver Nanoparticles. Silver nanoparticles were synthesized using the hydrogen reduction method.[13] Briefly, the

* To whom correspondence should be addressed. E-mail: gchumak@clemson.edu.
[†] Clemson University.
[‡] B.I. Stepanov Institute of Physics.

10.1021/jp900090a CCC: $40.75
Published on Web 04/03/2009

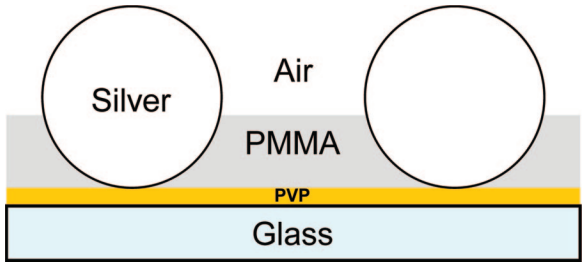

Figure 1. Schematic illustration of a side profile view of SNPs adsorbed on a glass microscope slide with PVP and the array immobilized with PMMA.

reaction was carried out in a round-bottom flask at 70 °C and pressurized to 10 psi with hydrogen gas. The size of the SNPs was controlled by the duration of the reaction. All SNPs used in this study were single crystals with a Feret's diameter of ca. 120 nm.

Fabrication of SNP Arrays. Microscope slides were cut into 12 mm × 12 mm sized pieces followed by sonication in water for 30 min, drying with a stream of nitrogen gas, and plasma treating for 5 min. The cleaned slides were placed into a 0.01% PVP solution and rolled on a hot-dog-style roller for a minimum of 3 h. After the PVP exposure, ethanol and water rinses were used to remove weakly adsorbed PVP before placing the slides into an aqueous SNP suspension and rolling overnight. Slides with attached SNPs were rinsed with water followed by ethanol and then dipped into a PMMA solution for 5 min. After exposure to the PMMA solution, the slides were spun dry at 7000 RPM for 45 s. A schematic of the immobilized SNP arrays is presented in Figure 1.

Theoretical Modeling. The quasi-crystalline approximation (QCA) of the statistical theory of multiple scattering of waves was used to model the extinction spectra of partially ordered 2D arrays of SNPs.[14] This is a highly efficient approach for partially ordered arrangements of scatterers and had successfully been applied previously to metal[15,16] and dielectric[17] close-packed nanoparticle arrays. According to this approach, the lateral electrodynamic interactions between individual particles in the array were considered as the interference of multiply scattered waves in both the near and the far field regions. The resulting field at any point of space was a sum of multiply scattered waves from individual SNPs, including their relative phases. In addition to the incident field, each particle experienced the field produced by all waves multiply scattered by other particles. The spatial distribution of particles in the arrays determines the correlation effects for the electrodynamic interactions and was described statistically by the radial distribution function $g(r)$ calculated in the Percus−Yevick approximation for hard spheres.[18]

The optical density of a closely packed 2D array of spherical SNPs, which gives the ratio of the specularly transmitted intensity I to the intensity of the incident light I_0, was calculated from the expression[14]

$$D(\lambda) = -\log_{10}\left\{\frac{I}{I_0}\right\} = -\log_{10}\left\{\left|1 - \frac{\pi}{k^2}\sum_{l=1}^{\infty} n_0(2l+1)(c_l + d_l)\right|^2\right\} \quad (1)$$

where $k = 2\pi/\lambda$ is the wavenumber, l is the order of vector spherical harmonics used in the expansion of electromagnetic fields (such an expansion is most convenient for the arrays of spherical particles), and n_0 is the number of SNPs per unit area, i.e., particle surface concentration. The coefficients c_l and d_l describe the effects of coherent multiple scattering in a partially ordered planar array. They can be calculated from the system of linear equations that binds up the radial distribution function $g(r)$ and the Mie coefficients for individual nanoparticles (see the detailed expressions for c_l and d_l in refs 14 and 17). Thus, c_l and d_l are drastically dependent on the array topology, particle size, and concentration as well as on the refractive index of the surrounding medium.

In the frame of the applied method we simulated a change in the SNPs' surrounding medium, which was caused by forming the PMMA layer between the individual SNPs in the arrays, by introducing the effective refractive index with the value intermediate between those of air and the PMMA and dependent on the PMMA thickness. Note, this approach did not account for irradiation of SNPs by evanescent waves reflected from air/PMMA or PMMA/substrate interfaces. All calculations in the paper were made using the silver optical constants taken from ref 19.

Results and Discussion

Stabilization of SNP Arrays with PMMA Layer. When unstabilized SNP arrays are dried, the particles undergo aggregation due to the surface tension forces associated with drying water (Figure 2a). The surface aggregation was an irreversible process, and the particles remained aggregated upon rewetting the arrays. In order to prevent surface aggregation, the particles were physically immobilized by casting a layer of PMMA between the particles (Figure 2b). Note, chemical attachment of particles does not prevent particles from 'rolling' on the surface and forming aggregates. The thickness of the PMMA layer is governed by the spin-drying speed and the PMMA concentration: the higher the concentration and the slower the spinning speed, the thicker the PMMA layer. The spinning speed was the most critical factor in fabricating consistently uniform layers. All substrates were spun dried at 7000 rpm because speeds lower than 7000 rpm resulted in nonuniform coverage. Electron microscope images of SNP arrays spun dried at different speeds revealed that the spinning speed did not affect the interparticle distance (data not shown).

Atomic force microscopy (AFM) was used for measuring the thickness of PMMA between the individual SNPs in the arrays. Figure 3 illustrates the effects of changing the concentration of PMMA at a constant spinning speed 7000 rpm. When 0.1% PMMA concentration was used, the layer was too thin to be reliably measured with AFM because its thickness was most likely smaller than the deviation of the particle size (Figure 3a); thus, the layer thickness was estimated to be a few nanometers at this concentration. The concentration of 1.0% resulted in a ∼15 nm thick layer (Figure 3b), 3.0% yielded the thickness of ∼90 nm (Figure 3c), and 5.0% PMMA completely filled the space between the SNPs (Figure 3d).

An important question is whether or not PMMA adsorbs to the surface of SNPs and remains there after spin drying. Even though PMMA does not contain functional groups that interact with silver, it was still possible that a thin layer of PMMA coated the particles via physiosorption. This layer could passivate the silver surface, preventing its direct accessibility to molecules of interest in potential sensing applications. In order to test the possibility for the interaction between PMMA and silver, the polymer was spun coated onto plain glass slides that were then immersed into a SNP suspension. The overnight exposure to SNPs did not result in any particles adsorbed to the slides,

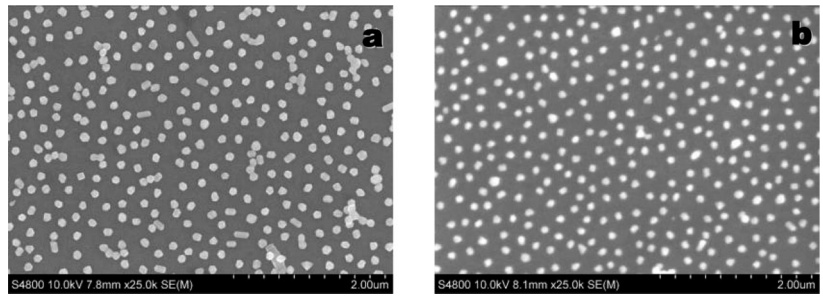

Figure 2. SEM images of dried silver nanoparticle arrays (a) without PMMA treatment and (b) treated with 5% PMMA solution.

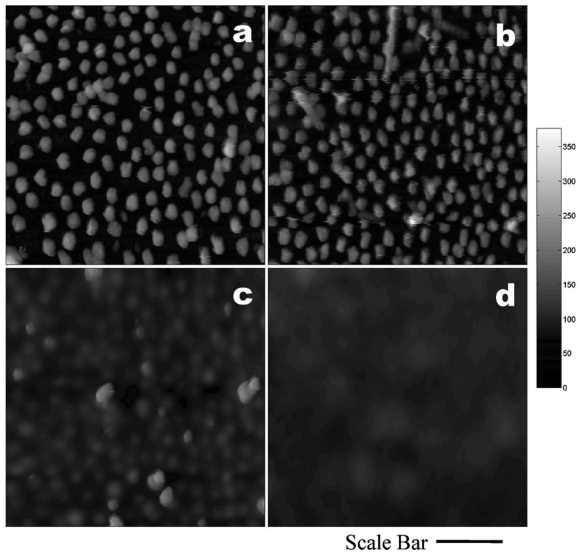

Figure 3. AFM images of silver nanoparticle arrays treated with (a) 0.1%, (b) 1%, (c) 3%, and (d) 5% PMMA solutions. Scale bar corresponds to 500 nm.

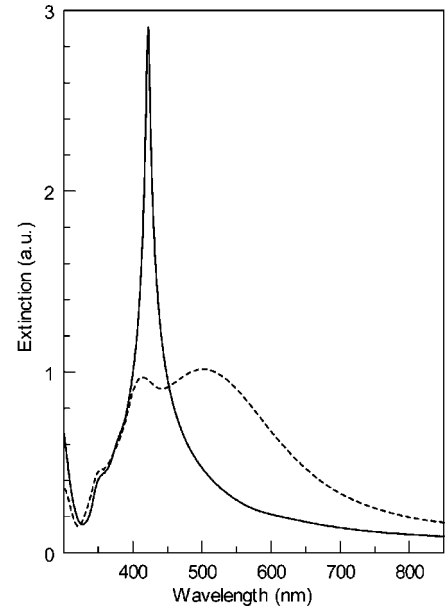

Figure 4. Extinction spectra of a strongly coupled 2D array of silver nanoparticles in water (solid) and aqueous suspension of SNPs (dash).

indicating the lack of an interaction between the two. In a different experiment, SNP arrays spun dried with 2% PMMA were exposed to a 1.0 mM 4-aminothiophenol solution for 30 min and exposed overnight to a SNP suspension. The 4-aminothiophenol molecule contains thiol and amino groups both capable of bonding to silver, and the formation of a second layer of SNPs was expected on the immobilized particles. Indeed, electron microscopy revealed from one to three additional SNPs adsorbed to every immobilized particle in the arrays (data not shown). On the basis of these experiments, it was concluded that the surface of the silver nanoparticles in the arrays was not covered with a PMMA layer after spin drying.

Effect of the Dielectric Medium on Plasmon Coupling. The coherent plasmon coupling in 2D arrays of SNPs was manifested as a characteristic sharp and intense band in the blue spectral range of the extinction spectrum (Figure 4) representing the coherent plasmon mode.[10] The same SNPs in aqueous suspension exhibit two maxima in the extinction spectra at 502 and 415 nm due to the dipole and quadrupole components of the plasmon resonance, respectively. It was experimentally demonstrated by stretching the coupled SNP arrays that the sharp band evolved from the quadrupole component of the plasmon resonance of noninteracting particles.[10] The immobilization of the arrays with PMMA layers provided an opportunity for studying the effect of the dielectric function in the space between the particles on the plasmon coupling.

The effect of the local dielectric function on the plasmon resonance of individual particles is well understood: the polarizability of the particles increases and the resonance shifts to the red spectral region in the media with higher dielectric function.[20−22] This behavior is commonly rationalized in terms of the screening charges induced in the polarizable medium in the close proximity to the particle.[22−24] The charges produce the 'restoring force' to the oscillating electrons, thereby affecting the frequency and intensity of the plasmon resonance. Higher dielectric function means larger polarizability of the medium and stronger restoring force causing the frequency shift to lower energies. The same argument is applied to plasmon coupling between particles: the dielectric medium shields the local field; therefore, the coupling should be reduced in media with a higher dielectric function.[22−24]

However, the current experiments revealed a different behavior: the strength of the coupling between SNPs in 2D arrays increased in the medium with higher dielectric function. As the PMMA concentration was increased from 0.05% to 5.0%, the effective refractive index in the space between particles increased from that close to 1.0 (air) to ca. 1.49 (PMMA),[25−27] and the arrays became progressively more coupled, reaching the maximum coupling when the spaces between the particles were completely filled with PMMA. The maximum coupling was concluded based on the observation of the sharpest and most intense plasmon band in the extinction spectrum of the arrays (Figure 5a). The experimental spectra agree well with the results of the numerical simulations presented in Figure 5b. One can see that increasing PMMA thickness lead to the same effect in extinction spectra as the immersion in water (discussed

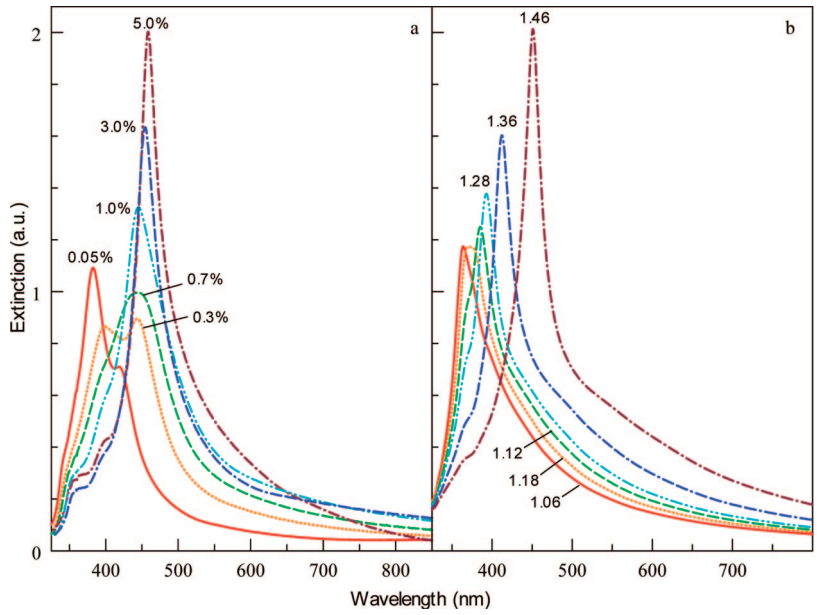

Figure 5. Experimental (a) and calculated (b) extinction spectra of silver nanoparticle arrays treated with 0.05% (solid), 0.3% (dot), 0.7% (dash), 1.0% (dot-dot-dash), 3.0% (dot-dash-dash), and 5.0% (dot-dash) PMMA solutions and measured in air. Calculated spectra correspond to the following values of effective medium refractive index: 1.06 (solid), 1.12 (dot), 1.18 (dash), 1.28 (dot-dot-dash), 1.36 (dot-dash-dash), and 1.46 (dot-dash). SNPs' surface concentration n_0=2.48 × 10^7 particles per mm^2.

below): the surface plasmon band moves to the red spectral region and becomes narrower.

The intensity of the quadrupole component in the measured spectra exhibited a nonmonotonic (having a minimum) dependence on the PMMA thickness (see Figure 5a). This behavior can be explained by the combined action of the two competing processes: the increase of the PMMA thickness decreased the free surface of SNPs that leads to reduced intensity of near field waves reflected from the glass substrate and, in this way, results in reduced intensity of the excited quadrupole mode (since the evanescent waves better excite the higher order modes upon irradiation of the metal nanoparticles).[28,29] However, when the interparticle space gets sufficiently filled with PMMA, plasmon coupling becomes sufficiently strong to turn this dependence: the intensity of quadrupole modes starts to increase due to exposure of particles to essentially nonuniform effective field.

Whereas the spectra in Figure 5a were measured in air, the same measurements were also performed with the arrays immersed in water. As expected, water increased coupling for the arrays that were not completely filled with PMMA: the arrays treated with 0.05% PMMA did not exhibit pronounced coupling in air but became strongly coupled in water (Figure 6a). On the other end, the arrays that were completely filled with PMMA and already displayed the sharp band did not show any spectral changes upon immersion in water (Figure 6d). The intermediate PMMA concentrations produced various degrees of spectral changes from dry to wet states (Figure 6b and 6c). As the PMMA layer thickness increased, the arrays became less sensitive to the changes of the dielectric function of the surrounding medium.

It was determined in previous work that plasmon coupling in 2D arrays of SNPs strongly depends upon the interparticle distance.[10] This dependence provides an opportunity to change the degree of the coupling by changing the particle surface coverage. Noncoupled and weakly coupled arrays were fabricated in this way, in addition to strongly coupled arrays described above, and the effect of the dielectric medium on their optical properties was studied. The particle surface coverage was varied by changing the concentration of SNPs in suspension

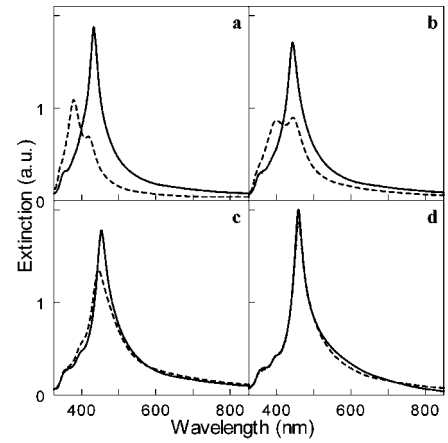

Figure 6. Extinction spectra of silver nanoparticle arrays treated with (a) 0.1%, (b) 1.0%, (c) 3.0%, and (d) 5.0% PMMA solution and measured in air (dash) and water (solid)

and/or by varying the exposure time. The films were treated with 0.05% of PMMA, and extinction spectra were measured in air and water. Upon immersion in water, the uncoupled films exhibited only red shifts of both quadrupole and dipole components of the plasmon resonance. The extinction spectra of these films resembled that of SNPs in suspension (Figure 7a). No significant coupling was observed in this case because the interparticle distances were too large for the overlap of the local electromagnetic fields from adjacent SNPs. The 20 nm red shift of the dipole component of the arrays in water as compared to the SNPs in suspension was due to the underlying glass substrate. The weakly coupled films exhibited an opposite behavior upon immersion in water: a 16 nm blue shift and sharpening of the plasmon resonance (Figure 7b). The blue shift and the sharpening of the resonance relative to those of the SNPs in suspension are indicative of the coherent plasmon coupling. This result further emphasizes the conclusion that increasing the dielectric function of the surrounding medium promotes the plasmon coupling in 2D arrays.

Tanabe[30] has shown using theoretical modeling that the intensity of the local electromagnetic field around SNPs is

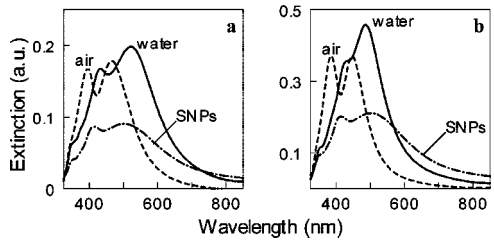

Figure 7. Extinction spectra of uncoupled (a) and partially coupled (b) silver nanoparticle arrays treated with 0.05% PMMA solutions and measured in air (dash) and water (solid). Dot-dash line corresponds to the extinction spectrum of silver nanoparticles in aqueous suspension and provided for reference.

enhanced in the media with higher refractive index, and the enhancement (E) can be calculated by

$$E = \left|1 + \frac{\alpha}{2\pi r^3}\right|^2 \quad (2)$$

The enhancement originates from the increased polarizability of the nanoparticles in a larger refractive index medium. The polarizability of the particle can be calculated using

$$\alpha = 4\pi a^3 \frac{\varepsilon_1 - \varepsilon_m}{\varepsilon_1 + 2\varepsilon_m} \quad (3)$$

where ε_1 and ε_m are the dielectric functions of the metal nanoparticles and surrounding medium, respectively. Equation 2 shows that the field enhancement is proportional to the square of the polarizability of the silver nanoparticle. In order to maximize the polarizability of the metal particle in the surrounding medium, $\varepsilon_{real} = -2\varepsilon_m$ must be satisfied so that $\varepsilon_1 + 2\varepsilon_m$ becomes small (where ε_{real} is the real component of the complex dielectric function of the metal nanoparticles). As ε_m is increased the plasmon resonance shifts to the red spectral range, where the absolute value of ε_{real} of the metal is also larger. However, the absolute value of ε_{real} becomes larger faster than ε_m, resulting in the numerator in eq 3 to increase and, consequently, leading to larger particle polarizability in media with larger ε_m. Larger particle polarizability leads to a stronger local electromagnetic field that, in turn, facilitates interaction with the neighboring particles. Therefore, the plasmon coupling between SNPs in 2D arrays increased and the resonance became sharper in the media with a larger dielectric function.

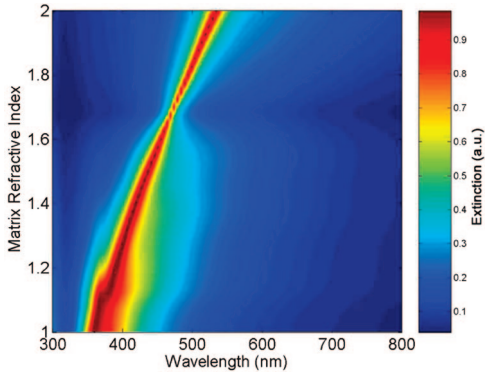

Figure 8. Normalized extinction maps of 2D SNP arrays as a function of matrix refractive index and wavelength ($n_0 = 2.48 \times 10^7$ particles per mm^2).

Our theoretical modeling also supports stronger coupling in 2D SNP arrays upon increasing the dielectric function of the surrounding medium. The results of the modeling are shown in Figure 8 as a map calculated for a range of the refractive index between 1.0 and 2.0. Increasing of the refractive index of the matrix sharpens and red shifts the plasmon peak, and the result commensurates with the experimental data in Figure 5a. The modeling results also indicate that there is an optimum refractive index of the matrix that produces the strongest plasmon coupling and the highest quality coherent plasmon mode.

Conclusion

Immobilization of SNP arrays with a thin PMMA layer provides a convenient method for stabilizing particles against surface aggregation and preserving their original arrangement. This method provided the opportunity for studying plasmon coupling, specifically how it is affected by the dielectric medium in the space between the particles. On the basis of experimental data and theoretical modeling, it was concluded that the plasmon coupling is more efficient in the media with higher dielectric function. Employing the quasicrystalline approximation method, the optimum refractive index of the medium was calculated, which results in the sharpest coherent plasmon mode with the highest quality factor.

Acknowledgment. The authors are grateful for the financial support from the United States Department of Energy, grant no. DE-FG02-06ER46342, and from the Belarusian Republican Foundation for Fundamental Research, grant no. F07M-228. We also thank Zack Gosser for synthesizing the silver nanoparticles used in this study and Craig Szymanski for processing AFM data using MatLab.

References and Notes

(1) Kreibig, U.; Vollmer, M. *Optical properties of metal clusters*; Springer: Berlin, New York, 1995.

(2) Dirix, Y.; Bastiaansen, C.; Caseri, W.; Smith, P. Oriented pearl-necklace arrays of metallic nanoparticles in polymers: A new route toward polarization-dependent color filters. *Adv. Mater.* **1999**, *11* (3), 223+.

(3) Knoll, W. Interfaces and thin films as seen by bound electromagnetic waves. *Annu. Rev. Phys. Chem.* **1998**, *49*, 569–638.

(4) Haynes, C. L.; McFarland, A. D.; Zhao, L. L.; Van Duyne, R. P.; Schatz, G. C.; Gunnarsson, L.; Prikulis, J.; Kasemo, B.; Kall, M. Nanoparticle optics: The importance of radiative dipole coupling in two-dimensional nanoparticle arrays. *J. Phys. Chem. B* **2003**, *107* (30), 7337–7342.

(5) Daniels, J. K.; Chumanov, G. Nanoparticle-mirror sandwich substrates for surface-enhanced Raman scattering. *J. Phys. Chem. B* **2005**, *109* (38), 17936–17942.

(6) Freeman, R. G.; Grabar, K. C.; Allison, K. J.; Bright, R. M.; Davis, J. A.; Guthrie, A. P.; Hommer, M. B.; Jackson, M. A.; Smith, P. C.; Walter, D. G.; Natan, M. J. Self-Assembled Metal Colloid Monolayers - an Approach to Sers Substrates. *Science* **1995**, *267* (5204), 1629–1632.

(7) Li, D. G.; Chen, S. H.; Zhao, S. Y.; Hou, X. M.; Ma, H. Y.; Yang, X. G. Simple method for preparation of cubic Ag nanoparticles and their self-assembled films. *Thin Solid Films* **2004**, *460* (1−2), 78–82.

(8) Hao, E.; Li, S. Y.; Bailey, R. C.; Zou, S. L.; Schatz, G. C.; Hupp, J. T. Optical properties of metal nanoshells. *J. Phys. Chem. B* **2004**, *108* (4), 1224–1229.

(9) Evanoff, D. D.; White, R. L.; Chumanov, G. Measuring the distance dependence of the local electromagnetic field from silver nanoparticles. *J. Phys. Chem. B* **2004**, *108* (5), 1522–1524.

(10) Malynych, S.; Chumanov, G. Light-induced coherent interactions between silver nanoparticles in two-dimensional arrays. *J. Am. Chem. Soc.* **2003**, *125* (10), 2896–2898.

(11) Malynych, S.; Robuck, H.; Chumanov, G. Fabrication of two-dimensional assemblies of Ag nanoparticles and nanocavities in poly(dimethylsiloxane) resin. *Nano Lett.* **2001**, *1* (11), 647–649.

(12) Malynych, S.; Chumanov, G. Coupled planar silver nanoparticle arrays as refractive index sensors. *J. Opt. A: Pure Appl. Opt.* **2006**, *8* (4), S144−S147.

(13) Evanoff, D. D.; Chumanov, G. Size-controlled synthesis of nanoparticles. 1. "Silver-only" aqueous suspensions via hydrogen reduction. *J. Phys. Chem. B* **2004**, *108* (37), 13948–13956.

(14) Hong, K. M. Multiple-scattering of electromagnetic-waves by a crowded monolayer of spheres - Application to migration imaging films. *J. Opt. Soc. Am.* **1980**, *70* (7), 821–826.

(15) Kachan, S. M.; Ponyavina, A. N. Spectral properties of close-packed monolayers consisting of metal nanospheres. *J. Phys.: Condens. Matter* **2002**, *14* (1), 103–111.

(16) Kachan, S.; Stenzel, O.; Ponyavina, A. High-absorbing gradient multilayer coatings with silver nanoparticles. *Appl. Phys. B: Lasers Opt.* **2006**, *84* (1−2), 281–287.

(17) Ponyavina, A.; Kachan, S.; Sil'vanovich, N. Statistical theory of multiple scattering of waves applied to three-dimensional layered photonic crystals. *J. Opt. Soc. Am. B* **2004**, *21* (10), 1866–1875.

(18) Throop, G. J.; Bearman, R. J. Numerical solutions of Percus-Yevick equation for hard-sphere potential. *J. Chem. Phys.* **1965**, *42* (7), 2408–2411.

(19) Palik, E. D. Handbook of Optical Constants of Solids. *Handbook of Optical Constants of Solids*; Academic Press: Orlando, FL, 1985.

(20) Jensen, T. R.; Duval, M. L.; Kelly, K. L.; Lazarides, A. A.; Schatz, G. C.; Van Duyne, R. P. Nanosphere lithography: Effect of the external dielectric medium on the surface plasmon resonance spectrum of a periodic array of sliver nanoparticles. *J. Phys. Chem. B* **1999**, *103* (45), 9846–9853.

(21) Novo, C.; Funston, A. M.; Pastoriza-Santos, I.; Liz-Marzan, L. M.; Mulvaney, P. Influence of the medium refractive index on the optical properties of single gold triangular prisms on a substrate. *J. Phys. Chem. C* **2008**, *112* (1), 3–7.

(22) Jain, P. K.; Eustis, S.; El-Sayed, M. A. Plasmon coupling in nanorod assemblies: Optical absorption, discrete dipole approximation simulation, and exciton-coupling model. *J. Phys. Chem. B* **2006**, *110*, 18243–18253.

(23) Choi, B. H.; Lee, H. H.; Jin, S. M.; Chun, S. K.; Kim, S. H. Characterization of the optical properties of silver nanoparticle films. *Nanotechnology* **2007**, *18* (7), .

(24) Sih, B. C.; Wolf, M. O. Dielectric medium effects on collective surface plasmon coupling interactions in oligothiophene-linked gold nanoparticles. *J. Phys. Chem. B* **2006**, *110*, 22298–22301.

(25) Andreas, B.; Breunig, I.; Buse, K. Modeling of X-ray-induced refractive index changes in poly(methyl methacrylate). *Chemphyschem* **2005**, *6* (8), 1544–1553.

(26) Kasarova, S. N.; Sultanova, N. G.; Ivanov, C. D.; Nikolov, I. D. Analysis of the dispersion of optical plastic materials. *Opt. Mater.* **2007**, *29* (11), 1481–1490.

(27) XiaoMing, T.; JianMing, Y.; HwaYaw, T.; Demokan, M. S. Modulation of refractive index and thickness of poly(methyl methacrylate) thin films with UV irradiation and heat treatment. *Appl. Surf. Sci.* **2005**, *252* (5), 1283–1292.

(28) Gluodenis, M.; Foss, C. A. The effect of mutual orientation on the spectra of metal nanoparticle rod-rod and rod-sphere pairs. *J. Phys. Chem. B* **2002**, *106* (37), 9484–9489.

(29) Quinten, M.; Pack, A.; Wannemacher, R. Scattering and extinction of evanescent waves by small particles. *Appl. Phys. B: Lasers Opt.* **1999**, *68* (1), 87–92.

(30) Tanabe, K. Field Enhancement around Metal Nanoparticles and Nanoshells: A Systematic Investigation. *J. Phys. Chem. C* **2008**, *112* (40), 15721–15728.

JP900090A